Polarisation Development at the European Spallation Source

Wai Tung Lee[1*], *Joel* Hagman[1], *Damian* Martin Rodriguez[1], *Annika* Stellhorn[1,2], *Alex* Backs[1,2], *Thomas* Arnold[1,3], *Elizabeth* Blackburn[2], *Pascale* Deen[1], *Celine* Durniak[1], *Mikhail* Feygenson[1,4,5], *Alexander* T. Holmes[1], *Judith* Houston[1], *Sebastian* Jaksch[1,4], *Oliver* Kirstein[1], *Dan* Mannix[1], *Martin* Månsson[6], *Manuel* Morgano[1], *Gøran* Nilsen[3], *Daria* Noferini[1], *Tommy* Nylander[2], *Dmytro* Orlov[2], *Valentina* Santoro[1], *Søren* Schmidt[1], *Michael* Schulz[7], *Werner* Schweika[1,4], *Markus* Strobl[8], *Aureliano* Tartaglione[1,7] , *Rasmus* Toft-Petersen[1,9], *Félix J.* Villacorta[1,10], *Peter* Willendrup[1,9], *Maximillian* Wolff[5], and *Robin* Woracek[1].

[1]European Spallation Source ERIC, 224 84 Lund, Sweden
[2]Lunds Universitet, 221 00 Lund, Sweden
[3]ISIS Neutron and Muon Source, STFC, Didcot, OX11 0QX, UK
[4]Forschungszentrum Jülich, D-52425 Jülich, Germany
[5]Uppsala Universitet, 751 05 Uppsala, Sweden
[6]KTH Royal Institute of Technology, SE-100 44 Stockholm, Sweden
[7]Technische Universität München, 85747 Garching, Germany
[8]Paul Scherrer Institut, 5232 Villigen PSI, Switzerland
[9]Technical University of Denmark, 2800 Kongens Lyngby, Denmark
[10]ESS Bilbao, 48160 Derio, Spain

Abstract. To meet the ever-increasing user demand, eleven of the fifteen European Spallation Source (ESS) instruments under construction aim to offer polarised neutrons for user experiments. They include an imaging instrument, a SANS instruments, two reflectometers, three diffractometers, and four spectrometers. In conjunction with in-kind contributions and instrumentation grants, the ESS Polarisation Project will support the incorporation of polarisation analysis on eight of the eleven instruments. The project aims to deliver polarised neutrons for first-science experiments as instruments enter operation. Different polariser and polarisation analyser techniques will be available to accommodate the specifics of experiments on a given instrument. Polarised ^{3}He neutron spin filter using either Metastable Optical Pumping (MEOP) or Spin-Exchange Optical Pumping (SEOP) techniques will provide shared-use equipment among many instruments, with SEOP's main application being *in situ* beam-polarisation. Several instruments will also use polarising-supermirror devices. To provide wide-bandwidth spin-flipping capability to the time-of-flight instruments, Adiabatic Fast Passage (AFP) neutron spin flippers, also known as gradient-field radio-frequency spin flippers will be the main method of choice. Devices based on the same AFP principle will also be used to flip ^{3}He nuclear spins. We are constructing our first ^{3}He polariser setup, including field coils to produce highly uniform magnetic field. Monte Carlo simulations are being done for the supermirror polarisers. To ensure science-focused development, we are working with university partners in doing scientific experiments with polarised neutrons. These are some of the activities developing polarisation analysis for ESS instruments in our project.

1 Introduction

Polarised neutrons are used extensively to study magnetism: in diffraction to study atomic-scale magnetic densities [1] and structures, Small Angle Neutron Scattering (SANS) to investigate magnetic nano-scale structures [2], reflectometry to probe magnetic multilayers and interfaces [3], spectroscopy to study magnetic dynamics [4], imaging to observe buried magnetic domains, mesoscopic structures and magnetic field distributions [5], and magnetic contrast in reflectometry is instrumental for solving the inverse-problem to obtain depth profiles directly with minimal use of modelling [6, 7]. Polarised neutrons have also proven to be an important complementary tool to deuteration, leading to accurate separation of coherent from spin-incoherent scattering, thereby separating coherent motion from single-particle motion [8]. Understanding these motions is of outmost importance for the field of sustainable energy materials, e.g., H-storage, rechargeable batteries, photovoltaic materials. In addition, the investigation of dynamical processes greatly benefits from the capabilities of high-resolution Neutron Spin Echo spectroscopy [9]. In fundamental physics, the search for the neutron electric dipole moment, the study of symmetry violation, and neutron life-time measurement are some of the topics that use polarised neutrons.

Neutron facilities have a long history of supporting their users' research by providing polarised neutrons. There has been a doubling of this capacity in the past two decades. This expansion continues: in existing

* Corresponding author: waitung.lee@ess.eu

facilities, 25 new and 13 existing unpolarised instruments plan to include polarised neutron capabilities. Together with 12 ESS instruments, there will be 50 more instruments around the world equipped with polarised neutron capabilities in the next 10 to 15 years. This increase is driven by increasing user demand, which in turn can be accounted for by the broader availability of polarised neutron technology, the two reinforcing each other in a virtuous cycle.

Few instruments had polarised neutrons capabilities in the early 1990s. This was due both to the relatively low neutron flux available for intensity-limited polarised neutron applications and to the limitations of the polarised neutron technology to accommodate experimental and instrumentational requirements. Since then, advances in polarising supermirror technology [10–12] – higher m-values, stacked supermirrors, and more complex geometries have expanded the energy range, angular divergence, and beam cross-section while reducing the length of the devices. At the same time, polarised ^{3}He neutron spin filter techniques have evolved far beyond the polarisation threshold and production volume required for scattering applications. Metastable Optical Pumping (MEOP) has achieved high throughput at high polarisation [13]. *In situ* Spin Exchange Optical Pumping (SEOP) was developed to continuously polarise the ^{3}He gas in the spin filter on the neutron beam. It keeps the neutron polarisation and transmission of the spin filter a constant during an experiment [14, 15]. Implementation of a nuclear magnetic resonance technique called "Adiabatic Fast Passage" (AFP) to change the ^{3}He polarisation with high efficiency [14, 15] allows the selection of the transmitted neutron spin state over almost any neutron energies. These continuous technological advancements have transformed polarised neutrons from a scarce to a widely available resource.

The increase in polarised neutron usage can also be quantified to some extent by searching a range of keywords relevant to polarised neutron in Google Scholar. The search results are only indicative and not an exact counting of publications that reported studies using polarised neutrons. The results nonetheless show a trend in the increasing use of polarised neutrons in research. Between the year 1999 and 2019, the polarised neutron scattering keywords hit-count almost tripled to 889 while "neutron scattering" hit-count almost doubled to 12800. Polarised neutron usage has outpaced the increase in using neutron scattering. While polarised neutron publications amount to 7% of neutron scattering publications, a significant number of them are published in high-impact journals. This is not a coincidence; the unique ability of polarised neutrons is often used to address the most difficult scientific questions that cannot be resolved using other techniques, resulting in a higher impact of polarised neutron publications.

2 Instruments with polarised neutrons

The ESS embraces a road map that will see twelve of the fifteen instruments that are currently under construction [16], have polarised neutron beam capabilities [17].

Polarisation components for the MAGiC diffractometer, the ESTIA reflectometer and the T-REX spectrometer are fully included in their in-kind instrument construction projects. They all involve using polarising supermirrors, and T-REX will also use polarised ^{3}He devices. The details of these instruments are given in another article [16] and not covered in this article.

Table 1. ESS instruments with polarised neutron option.

Class	Name	Application
Diffractometer	DREAM	Bispectral diffraction + nm-SANS
	HEIMDAL	Hybrid diffraction + SANS + Imaging
	MAGiC	Magnetism single-crystal diffractometer
Imaging	ODIN	Imaging
Reflectometer	ESTIA	Polarised neutron focusing reflectometer
	FREIA	Liquids reflectometer
SANS	SKADI	SANS (magnetism + soft-matter)
Spectrometer	BIFROST	Extreme environment spectrometer
	CSPEC	Cold chopper spectrometer
	MIRACLES	Backscattering spectrometer
	T-REX	Bispectral chopper spectrometer

This article focuses on the ESS Polarisation Project, which will provide polarisation components to the other eight instruments in conjunction with in-kind contributions to the SKADI polariser, a grant-supported DREAM polariser by the DREAM team, a grant supporting ODIN, SKADI and LoKI polarised instrumentation, and a grant for BIFROST and CSPEC analysers.

The characteristics of each instrument, the characteristics of the available technologies for polariser, analyser, and spin-flipper, and the requirements of the spin-transport and sample magnetic field, determine the layout and configuration of the polarisation setup. A detailed evaluation of the equipment choices however, is not the focus of this article. Here we focus on specifying the polarisation instrumentation for the nine instruments in the project and providing an update on some of the developments.

It is important that the needs for scientific experiments should guide the instrumentation development. In this project, we have been engaging researchers in universities to carry out scientific studies

using polarised neutrons in other neutron facilities. In particular, our collaborations have reported both polarised SANS and polarised imaging studies in this conference [18, 19]. In carrying out these experiments, the experimental needs have informed the designs of the polarisation setup for our instruments. In return, our instrumentation knowhow and capabilities have assisted in both analysing the measurement data and developing the experimental setup.

2.1 Diffractometers

The DREAM [20] and HEIMDAL [16] neutron powder diffractometers have complementary science cases, with design features suitable for adopting similar polarization equipment. The wavelength band of both instruments covers 0.5 Å to 4 Å and 4 Å to 10 Å, respectively, with the shorter wavelengths for diffraction and pair-distribution function measurements, and the longer wavelengths for SANS measurements, and in the case of HEIMDAL for imaging. DREAM features a low-angle scattering detector for covering limited q-range and suitable for nanoscale materials studies (nm-SANS), while the HEIMDAL SANS detector provides a conventional SANS q-coverage. The ^{3}He polariser for cold neutrons at DREAM is provided by a grant (see Acknowledgement). The thermal neutron polariser cell for DREAM and HEIMDAL will be provided by the ESS Polarisation Project. AFP is implemented in the ^{3}He polariser to select the neutron spin state. This method flips the ^{3}He polarisation and switches which neutron spin state is filtered. Polarising supermirror device for cold neutrons are currently being evaluated for both instruments.

Diffraction instruments have large detector coverage. SANS and imaging applications need to avoid background due to potential SANS scattering from supermirrors. Polarised ^{3}He spin filters are therefore best suited for the analyser for DREAM and HEIMDAL. The project will provide the analyser setup to both instruments. The wide-angle component will cover the large scattering angles in diffraction and a shorter cold neutron analyser will support SANS and imaging.

A coil set producing a 3D field with mT field strength will provide the uniform holding field for the ^{3}He analyser and allow the user to apply the field in any direction at the sample position. For diffraction, the technology to flip the analyser polarisation in a wide-angle analyser is currently not available, making it challenging to separate magnetic and nuclear scattering. The 3D field will allow the use of the "XYZ method" [21–23] to extract the magnetic scattering signals. Using finite-element field calculations, we have designed a coil set providing a large unobstructed angular range in both the horizontal and vertical directions.

The ^{3}He analyser for SANS and imaging has a narrower profile and can be placed further from the sample position. The AFP technique to flip the ^{3}He polarisation for such geometry is readily available.

2.2 Imaging instrument

At ODIN [16], a supermirror polariser will polarise the incoming beam where it enters the instrument cave. The polariser operates in a wavelength band from 2.5 Å to 11 Å. Despite the beam divergence at this location, Monte Carlo simulations using McStas [24, 25] show that a multi-channel v-cavity can deliver a beam with polarisation > 95% (see Fig. 1) and transmission > 40% (not shown, see the following referenced article) for an area of 10 cm × 10 cm at 5 m from the pinhole [26]. More calculations are underway to optimise the polariser to the beam geometry.

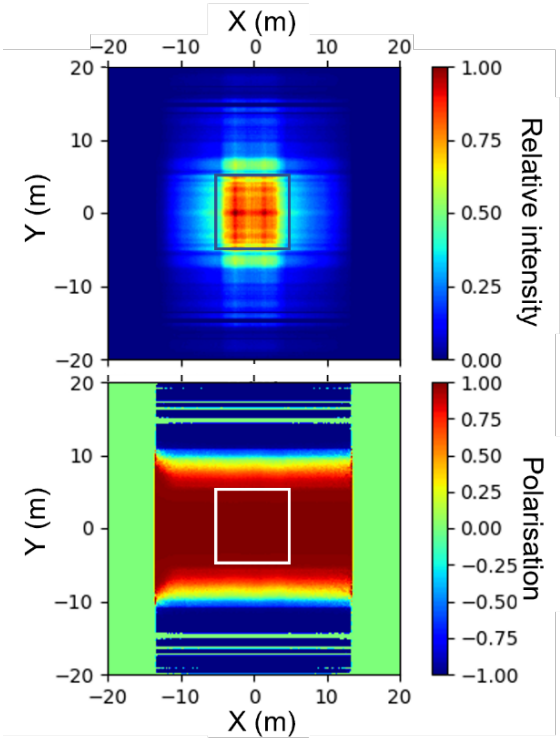

Fig. 1. ODIN polariser Monte Carlo simulation results showing (a) relative beam intensity normalise to the highest intensity value and (b) polarisation at 5 m from the pinhole. The beam is diverging at this location. A square is superposed to the figures to identify the centre 10 cm × 10 cm area. The beam has high intensity and the polarisation is > 95% in that area. Reference [26] gives the details of this simulation and also includes simulations for BIFROST and MIRACLES.

Other than the "remnant polariser" [27], a setup using a polarising supermirror device such as the ODIN polariser described above requires a neutron spin flipper to enable measurements with both spin+ and spin− states consecutively. Based on the same principle, an AFP neutron spin flipper [28] has a wide neutron wavelength working range and places no material in the neutron beam. It is hence a suitable choice for the ESS instruments and in particular for imaging.

To obtain the highest possible spatial resolution in neutron imaging, the sample is typically placed as close to the detector as possible. In polarised neutron imaging, the analyser has to be placed behind the sample and in order to minimise the sample-to-detector distance, a customised compact supermirror analyser that matches the beam characteristics will be made available.

To allow for further extension of the wavelength range, the guide fields will be designed to be highly uniform to accommodate a ^{3}He analyser. In addition, polarised imaging applications often use custom designed, application specific, spin manipulation equipment that requires precise control of the magnetic field. Using another uniform field compensation coil to enclose the spin manipulation components and applying a field in the opposite direction, the highly uniform guide field can be cancelled and thus preventing the guide field from interfering with the spin manipulation devices.

Polarised ^{3}He is susceptible to magnetic interference. This will restrict how close a magnetised sample in a sample field can be placed to the ^{3}He analyser and therefore to the detector. This in turn limits the spatial resolution of the measurements. Wolter optics [5, 29] is currently being developed at a number of facilities. It has many advantages, including the ability to focus a neutron beam at the detector. This will allow greater distances between the sample, the analyser and the detector without significantly degrading spatial resolution. Thereby allowing the full utilisation of the ^{3}He analyser.

2.3 Reflectometer

The main use for polarised neutrons on the FREIA reflectometer [16] is the magnetic reference layer technique [6, 7]. The wavelength band usually spans from 2 Å to 11.3 Å. The unique design of FREIA uses an elliptical guide to deliver a wide (around 3.5°) divergence to the sample, from which up to three collimated beams are selected in order to vary the incident angle without the need to move the sample. Since the polarised ^{3}He technique is considerably less sensitive to beam divergence, it is the preferred method for this instrument. An *in situ* SEOP polariser with AFP flipping of the ^{3}He polarisation will be used to keep the polarisation constant during an experiment. We will also investigate an analyser setup that can operate within the geometry of the scattered beam.

The magnetic reference layer method requires a sample field to manipulate the magnetisation of the reference layer. The location and magnetic shielding of the polariser, and the sample magnet design will prevent the magnetic fringing field from interfering with the polariser. There are also various steel components in some of the slits in the current collimation system design, which are close to the polarised beam. The effect on the spin-transport guide field has been investigated using finite-element magnetic field calculation which shows that strengthening the guide field at several locations will mitigate the interference to the polarised beam.

2.4 SANS instruments

The wavelength range for this project are similar for both SKADI [30] and LoKI [16], from 3 Å to 10 Å. SKADI will be the main polarised SANS instrument for users and comes with its own supermirror polariser and incident beam neutron spin flipper. While LoKI does not focus on polarisation in its application, the earlier commissioning of LoKI however allows us to test the polarisation equipment for SKADI in advance.

Both SANS instruments will use ^{3}He analysers to avoid background due to potential SANS scattering from supermirrors. There are two options provided: a uniform 3D field coil set that allows a large scattering angle for SANS, and a magnetostatic cavity that can work with a Tesla-range sample field will be provided for the analyser. The analyser will feature *in situ* SEOP to maintain a static analysing efficiency during an experiment. The selection of neutron spin state will be facilitated by AFP flipping of ^{3}He polarisation.

2.5 Spectrometers

The polarisation setup for three spectrometers, BIFROST [16], CSPEC [31], and MIRACLES [16] is supported by this project, with an additional grant partially supporting the polarisation setup on BIFROST and CSPEC. The shared polarised ^{3}He equipment can be used on T-REX if needed.

BIFROST will use polarising supermirrors for both its polariser and wide-angle analyser, which match the beam characteristic and geometry of the instrument. Both devices will be designed to cover an energy band from 2.3 meV to 13 meV. The polariser, a multi-channel v-cavity device will be located at the end of the straight section of an elliptical neutron guide at 19 m from the sample position. At this location, the neutron beam will have less than 0.2° divergence. Monte Carlo simulations using McStas show that a multi-channel v-cavity polariser can produce a beam with polarisation > 95% and transmission > 40% [26].

The polarisation analyser of BIFROST will accept ±14° vertical angle. It is therefore viable to use a supermirror analyser and benefit from the high transmission and analysing efficiency. The analyser is partially supported by a grant which supports the construction of a similar device at the ISIS Neutron and Muon Source in UK. A preliminary magnetic field calculation using finite element calculation software COMSOL Multiphysics [32] was performed to evaluate the uniformity and field strength required to magnetise the supermirrors.

CSPEC plans to use a supermirror polariser at a focusing part of the neutron guide. The design will focus on 3 Å to 10 Å neutrons. Given the large detector coverage, a ^{3}He wide-angle analyser will be used together with the 3D uniform field coil mentioned above. The grant mentioned above also supports the development of the wide-angle analyser.

The polarisation setup at MIRACLES is illustrated in Fig. 2. The polariser is located before the focusing section of its elliptical neutron guide at 19 m from the sample position. Likewise, we have used McStas to simulate the polariser and found that a v-cavity polariser will polarise neutrons at wavelengths longer than 5 Å with polarisation > 95% and transmission > 40% [26].

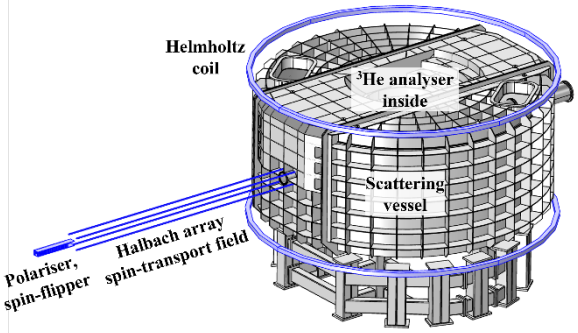

Fig. 2. Layout of MIRACLES polarisation setup. The analyser cell is located inside the sample chamber.

A ^{3}He wide-angle analyser will be located in the sample chamber and configured as a sample environment insert. The setup simplifies the setting up experiments without the need to break the vacuum in the scattering vessel. Helmholtz coils outside the scattering vessel will provide the magnetic field environment needed for the ^{3}He analyser and for spin-transport. Rather than placing the coils inside the scattering vessel, the placement avoids the issue of cooling large DC coils in the vacuum environment and potential interference with neutron flight paths by the coils' support structure.

To ensure neutron spin-transport from the polariser on MIRACLES, and similarly on BIFROST to their respective sample position 19 m away, Halbach array consisting of four lines of permanent magnets will provide the guide field along the neutron flight path.

2.6 Test beam line

The Test Beam Line is one of the instruments in the approved suit of ESS instruments. Besides several other tasks, it will provide a test bed for polarisation equipment. We are investigating the beam equipment that can be tested within the constraints of the instrument (the average length is ~3 m in front of the beam stop).

3 Shared polarised ^{3}He equipment

Polarised ^{3}He equipment can be shared among different instruments without sacrificing the performance. Shared devices are used in our design where it is applicable and beneficial.

3.1 Neutron spin filter

Polarised ^{3}He neutron spin filters are separated into two classes associated with the ^{3}He cell geometry: cylindrical cells and wide-angle cells.

Cylindrical cells are typically 5 cm to 15 cm in diameter and 5 cm to 15 cm in length. The neutron beam enters and exits the cell through the circular faces. The applications are polarisers, and analysers for SANS and imaging. The technology for using this device with *in situ* SEOP gas-polarising is well-developed and readily available [14, 15]. A majority of applications of cylindrical cells at the ESS will be *in situ* SEOP setup.

Without continuously polarising the gas, ^{3}He polarisation will decay over time, resulting in low neutron transmission and polarisation. Consider a polariser with an initial ^{3}He polarisation of 80%, at a selected wavelength where the neutron polarisation would be 90%, the unpolarised incident beam transmission would be 37%. If a similar analyser is used, the combined transmission would be 24% for the high-transmission spin state. If one of them has a decay time constant of 150 hours while the other is an *in situ* setup, the transmission would be 19% after 24 hours; a drop of 20% from the initial transmission. If both spin filters are *ex situ* setups, the transmission drops to 15% in 24 hours, i.e., a loss of 40% in transmission. To allow for no less than 19% transmission, both cells will need to be changed every 12 hours. Experiences show that an experiment would be interrupted between 15 minutes to a couple of hours in order to change to a newly polarised cell or batch of ^{3}He gas. The use of *in situ* SEOP setup, where it is applicable, would reduce such disruption to experiments.

The other class of cells are the wide-angle analyser cells to accommodate a large range of scattering angles in diffractometers and spectrometers. The cells consist of concentric arcs of glass walls with flat top and bottom. Scattered neutrons pass the curved walls and the volume of polarised ^{3}He gas inside. A typical cell has an inner diameter of 6 cm to 7 cm and an outer diameter of about 20 cm. The arc covers an angle between 90° to 160°. The cell height is 6 cm to 12 cm.

These cells typically work with *ex situ* gas polariser using a Metastable Optical Pumping (MEOP) filling station. A MEOP station is too large to be located on an instrument but has several other advantages. There are two modes of MEOP operation. In the cell-exchange mode, a spin filter cell is filled in the MEOP station, then taken to the instrument and exchanged with the cell in the instrument. In the gas-exchange – or what is known as "local filling" mode [33] – the gas in the spin filter cell in the instrument is exchanged with the newly polarised gas in a transport cell. While the cell-exchange method may be simpler when there is easy access to the location of the cell, it is difficult to access the cell at most ESS instruments that will use the wide-angle ^{3}He analyser. The more complex local-filling setup would be the method of choice. Despite the complexity in the setup, the local-filling method allows a shorter interruption to the experiment and have lower gas polarisation loss during the exchange.

Wide-angle SEOP cells have been developed in several facilities [34]. The polarising condition of 160 °C to 200 °C and the need to use laser along the field axis make it impractical for *in situ* application in close proximity to a sample or sample environment equipment. The cell seals in ^{3}He gas and SEOP requires at least 1 day to polarise a cell. This does not compare favourably to the MEOP method where the optimal gas pressure is chosen according to experimental needs and the significantly shorter 1 to 2 hours of gas-filling time. In addition, it is challenging to work with high-stress aluminosilicate glass to make SEOP cells. For these reasons, a majority of the existing wide-angle cells are MEOP based.

The ESS polarised ^{3}He neutron spin-filter line-up thus includes both *in situ* SEOP setup for a majority of

applications using cylindrical cell and MEOP setup for wide-angle analysis cells. There are some exceptions that use cylindrical cells but cannot use *in situ* SEOP. They will use the MEOP method. As a first step, a SEOP setup is being built to provide the platform for development and testing. And discussion is underway with the Institute Laue Langevin for a collaboration to construct a MEOP station.

3.2 Magnetic field device

^{3}He polarisation is highly susceptible to magnetic field gradients. The environment of the spin filter must be well controlled to minimise magnetic interference. In the case where an external field gradient cannot be eliminated, magnetic shielding made of high permeability materials such as μ-metal should be used to shield the ^{3}He cell.

First and foremost, the magnetic field device that provides the holding field to the ^{3}He cell must be highly uniform. At the cell, the angular gradient of the applied magnetic field would ideally be less than 2×10^{-4} rad/cm [35]. There are two main class of magnetic field devices for polarised ^{3}He applications: field coils and magnetostatic cavity.

Magnetostatic cavities are used with cylindrical cells, either as polariser or as analyser at a distance downstream from the sample. The μ-metal that is part of its constituents provides magnetic shielding to the ^{3}He cell, allowing the device to be used with Tesla-range sample magnets. The two most common cavity types are "Magic Box" [36] and solenoid [37]. In a magic box, field coils wrapped around μ-metal plates provide the magnetic flux. The flux is channelled by the μ-metal plates to produce a uniform field over the entire volume of the cell. The other type uses a compensated solenoid to produce the uniform field, where a μ-metal outer shell both improves the uniformity and serves as flux return.

3D uniform field coils are used with the sample environment at its centre. Uniform field coils have long been investigated and many configurations can be found in literature. Some of the existing coils used in ^{3}He spin filter applications are the "Pastis" coils [38, 39] and there are also hybrid approaches that use both coils and μ-metal plates to produce a 3D uniform field with large horizontal angular span [40, 41].

In our on-going development of uniform field coils, our design of a rectangular coil set has, thus far, reached a uniform-field volume of 22 dm^3 (Fig. 3a). This is larger than coils published in literature for rectangular coil sets with similar outer dimensions [42]. Two 15 cm diameter and 10 cm long ^{3}He cells, i.e., a polariser and an analyser, can be placed in the uniform field region at 10 cm to 12 cm apart, with space to spare.

Likewise, our coil design of circular coil sets for wide-angle scattering use has reached a uniaxial uniform volume 24 cm in diameter and 12 cm tall, with an unobstructed vertical angle at ±28° (Fig. 3b). In contrast, a similar coil called "tetracoil" [43], which is known for its large uniform volume, has a considerably smaller unobstructed vertical angle of ±17°. We know of no other published coil with similar performance.

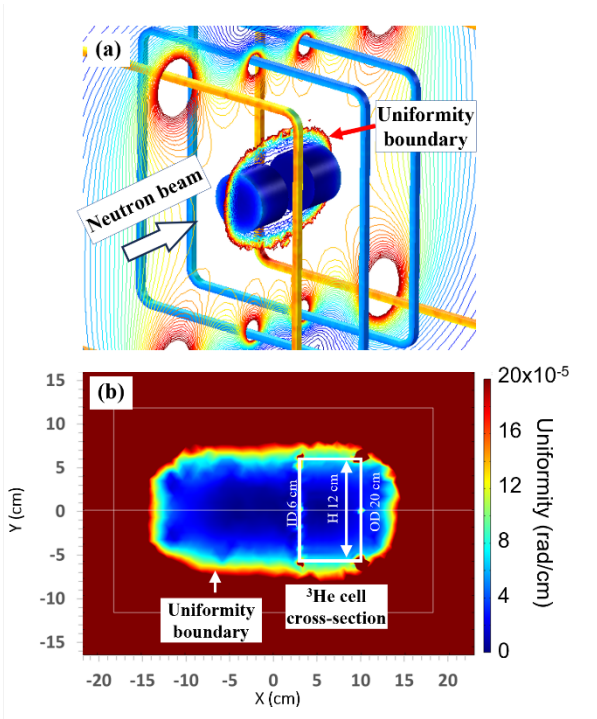

Fig. 3. Uniformity volume in our designs of (a) rectangular coil set, showing ^{3}He cells in their operation position, (b) circular coil set, showing the cross-section of a wide-angle cell. Within the red boundary, the uniformity is better than 2×10^{-4} rad/cm.

We have incorporated additional design to provide a 3D field. There is additional loss of vertical opening yet it still yields unprecedented performance. As this is an on-going work, the details of these coils are out of the scope of this overview article.

4 Polarised data processing

A major bottleneck in using polarised neutrons is data reduction. Several measurements of different incident and scattered spin states need to be reduced together, as oppose to unpolarised neutron measurements where each measurement is reduced independently. Without an appropriate tool to reduce the polarised data during an experiment, users cannot easily separate the effects due to finite neutron polarisation from sample magnetic scattering. The situation is even more complicated if polarised ^{3}He with changing polarisation is used.

The mathematics to reduce polarised data is readily available [44]. It applies across different scattering methods and can be automated. The key equation is

$$\bar{I} = \widehat{T^A}\ \widehat{F_2}\,\widehat{F_1}\,\widehat{T^P}\,\bar{S} \tag{1}$$

with $\bar{I}$ being the measured intensities,

$$\bar{I} = \begin{pmatrix} I_{++} \\ I_{+-} \\ I_{-+} \\ I_{--} \end{pmatrix} \tag{2}$$

and $\bar{S}$ being the intensities after polarisation data reduction,

$$\bar{S} = \begin{pmatrix} S_{++} \\ S_{+-} \\ S_{-+} \\ S_{--} \end{pmatrix} \quad (3)$$

where the first and second subscripts of + and – denote the neutron spin state before and after the sample, respectively. The matrices connecting $\bar{I}$ and $\bar{S}$ are:

Polariser transmission matrix,

$$\widehat{T^P} = \begin{pmatrix} T_+^P & 0 & T_-^P & 0 \\ 0 & T_+^P & 0 & T_-^P \\ T_-^P & 0 & T_+^P & 0 \\ 0 & T_-^P & 0 & T_+^P \end{pmatrix}; \quad (4)$$

Incident neutron spin-flipper transmission matrix, assuming spin+ neutrons are transmitted with the flipper off,

$$\widehat{F_1} = \begin{pmatrix} 1 & 0 & 0 & 0 \\ 0 & 1 & 0 & 0 \\ 1-F_1 & 0 & F_1 & 0 \\ 0 & 1-F_1 & 0 & F_1 \end{pmatrix}; \quad (5)$$

Scattered neutron spin-flipper transmission matrix, assuming spin+ neutrons are transmitted with the flipper off,

$$\widehat{F_2} = \begin{pmatrix} 1 & 0 & 0 & 0 \\ 1-F_2 & F_2 & 0 & 0 \\ 0 & 0 & 1 & 0 \\ 0 & 0 & 1-F_2 & F_2 \end{pmatrix}; \quad (6)$$

Analyser transmission matrix,

$$\widehat{T^A} = \begin{pmatrix} T_+^A & T_-^A & 0 & 0 \\ T_-^A & T_+^A & 0 & 0 \\ 0 & 0 & T_+^A & T_-^A \\ 0 & 0 & T_-^A & T_+^A \end{pmatrix}. \quad (7)$$

F_1 and F_2 in Equations 5 and 6 are the neutron spin-flipper efficiency before and after the sample, respectively. Their values are measured experimentally, with 0 being non-functioning and 1 being perfectly efficient. A properly designed flipper often has a high efficiency of more than 0.99.

For polarising supermirror devices, the transmission of spin+ and spin– states are given by

$$T_\pm = \frac{1 \pm E}{2} \quad (8)$$

where E is the polariser or analyser efficiency. $E = 1$ corresponds to perfect efficiency and $E = 0$ means the device is not spin-filtering neutrons. The efficiency is determined experimentally. Here we omit the designation of polariser P and analyser A for simplicity.

For polarised ^{3}He, the spin+ and spin– transmissions are given by

$$T_\pm = T_g \exp(-O \pm OP_{He}). \quad (9)$$

T_g is the neutron transmission of the cell body. Its value is measured experimentally. P_{He} is the ^{3}He polarisation and O is the ^{3}He opacity, given by

$$O = n\,\sigma_0\,\lambda\,l, \quad (10)$$

where n is the number density of ^{3}He gas in the cell. σ_0 *is* the absorption cross section of 1 Å neutron by ^{3}He, $\sigma_0 = 2966 \times 10^{-24}$ cm^2. λ is the neutron wavelength. l is the path length through the cell. Helium has the least deviation from the ideal gas law among all gases, with less than 0.1% deviation in density in standard conditions. We consider n to be related to the cell pressure p by the ideal gas law, given by $p = nk_BT$, with Boltzmann constant k_B and temperature T. A practical adaptation of Equation 10 is the follow equation:

$$O = 0.0733\,p\,l\,\lambda \quad (11)$$

where p is the cell pressure at 20 °C in bars, neutron wavelength λ is in Å and the path length l is in cm.

The path length l is known when the cell body is made. ^{3}He pressure p is measured when the cell is filled. Knowing the neutron wavelength λ in the measurement, the opacity O can be calculated from Equation 11.

During the experiment, ^{3}He polarisation P_{He} can be obtained by measuring unpolarised neutron transmission T_N and using the following equation to analyse the result:

$$T_N = T_g \exp(-O) \cosh(OP_{He}). \quad (12)$$

Subsequently one can calculate the spin filter's transmission matrices in Equations 4 and 7 and use Equation 1 to obtain the reduced data $\bar{S}$.

This formalism has been successfully applied to analyse polarised diffraction data measured using polarised ^{3}He neutron spin filters [45]. Working together with the data scientists at ESS' Data Management & Software Centre (DMSC), we intend to develop and incorporate the data reduction algorithm to the instrument data processing software so that users can reduce polarised data during the experiment.

In a number of publications, including the seminal article cited above, Equation 1 was incorrectly given as $\bar{I} = \widehat{F_1}\,\widehat{F_2}\,\widehat{T^P}\,\widehat{T^A}\,\bar{S}$. While the two spin-filter matrices commute, $\widehat{T^P}\,\widehat{T^A} = \widehat{T^A}\,\widehat{T^P}$, and the two spin-flipper matrices also commute, $\widehat{F_1}\,\widehat{F_2} = \widehat{F_2}\,\widehat{F_1}$, the polariser or analyser matrix and either spin flipper matrix do not, i.e. $\widehat{F_1}\,\widehat{T^P} \neq \widehat{T^P}\widehat{F_1}$ and so on. This error was not discovered earlier perhaps due to the fact that neutron spin flippers often have high efficiency. $\widehat{F_1}$ and $\widehat{F_2}$ are close to being a unit matrix so the error was small. The equation however gives unphysical results in some settings so it is important to use the correct formula.

5 Summary

In this article, we provide an overview of the polarised neutron instrumentation for nine ESS instruments supported by the Polarisation Project. We specified the equipment selected for each instrument and provided further information on the polarised ^{3}He equipment. Finally, we discussed polarised data reduction, especially the methodology when using polarised ^{3}He neutron spin filters.

Acknowledgements

The authors acknowledge the support from the following grants and in-kind project:

1. Support for DREAM polariser: Röntgen Ångström Cluster: nPDFSAS (grant no 2019-06117_VR). https://portal.research.lu.se/en/projects/npdfsas-simultaneous-polarized-sans-and-npdf-methods-to-study-nov
2. Support for ODIN, SKADI/LoKI polarisation: W.- T. Lee, E. Blackburn, T. Nylander, D. Orlov, J. Houston, S. Jaksch, M. Manual, C. Pappas, S. Schmidt, M. Schulz, M. Strobl, A. Tartaglione, R. Woracek, Tillväxtverket European Regional Development Fund project SREss3 (2020-2023).
3. Support for BIFROST, CSPEC polarisation: E. Blackburn, M. Månsson, W.-T. Lee, G. Nilsen, P. Deen, R. Toft-Petersen, M. Pascal, Swedish Research Council (VR) "Cooperation with ISIS: instrumentation and methods for ESS" Grant # 2021-06157.
4. Swedish Research Council (VR) : In-Kind Contribution to the ESS, "Neutron Polarisation Capability Development for User Experiment Applications on ESS Instruments", 2023-2025.

References

1. B. Gillon, P. Becker, *Magnetization Densities in Material Science,* in Modern Charge-Density Analysis, C. Gatti, P. Macchi, *ed*., Dordrecht, Springer, 277 (2011).
2. A. Wiedenmann, Physica B **356**, 246 (2005).
3. C. Majkrzak, Physica B **173**, 75 (1991).
4. L. Regnault, *Inelastic Neutron Polarization Analysis*, in Neutron Scattering from Magnetic Materials, Tapan Chatterji, *ed*., Elsevier Science, 363 (2006).
5. M. Strobl, H. Heimonen, S. Schmidt, M. Sales, N Kardjilov, A. Hilger, I. Manke, T. Shinohara, J. Valsecchi, J. Phys. D **52**, 123001 (2019).
6. T. Nylander, R. Campbell, P. Vandoolaeghe, M. Cárdenas, P. Linse, A. Rennie, Biointerphases **3**, FB64–FB82 (2008).
7. S. Holt, A. Le Brun, C. Majkrzak, D. McGillivray, F. Heinrich, M. Lösche and J. Lakey, Soft Matter **5**, 2576 (2009).
8. A. Arbe, G. J. Nilsen, J. R. Stewart, F. Alvarez, V. Sakai and J. Colmenero, Phys. Rev. Res. **2**, 022015 (2019).
9. F. Mezei, Z. Physik, **255**, 146 (1972).
10. P. Böni, Physica B **234-236**, 1038 (1997).
11. T. Krist, C. Lartigue, F. Mezei, Physica B **180-181**, 1005 (1992).
12. T. Bigault, G. Delphin, A. Vittoz, V. Gaignon, P. Courtois, J. Phys.: Conf. Ser. **528**, 012017 (2014) and references therein.
13. K. Andersen, R. Chung, V. Guillard, H. Humblot, D. Jullien, E. Lelièvre-Berna, A. Petoukhov, F Tasset, Physica B **356**, 103 (2005).
14. G. Jones, J. Baker, W.-C. Chen, B. Collett, J. Cowan, M. Dias, T. Gentile, C. Hoffmann, T. Koetzle, W.-T. Lee, K. Littrell, M. Miller, A. Schultz, W.M. Snow, X. Tong, H. Yan, A. Yue, Physica B **356**, 86 (2005).
15. W.-T. Lee, X. Tong, J. Pierce, M. Fleenor, A. Ismaili1, J. Robertson, W.-C. Chen, T. Gentile, A. Hailemariam, R. Goyette, A. Parizzi, V. Lauter, F. Klose, H. Kaiser, C. Lavelle, D. Baxter, G Jones, J. Wexler, L. McCollum, J. Phys.: Conf. Ser. **251**, 012086 (2010).
16. K. Andersen, *et. al*., Nucl. Instrum. Methods A **957**, 164302 (2020).
17. W.-T. Lee, A. Arbe, T. Arnold, E. Blackburn, S. Carretta, P. Deen, E. Lelièvre-Berna, S. Mattausch, G. Nilsen, C. Pappas, S. Schmidt, X. Tong, Report on ESS Polarisation Workshop, ESS-3549713 (2020).
18. A. Backs, S. Sebold, M. Busi, W.-T. Lee, M. Strobl, D. Orlov, *this proceeding* (2023).
19. A. Stellhorn, W.-T. Lee, E. Kentzinger, W.C. Chen, J. Gaudet, K. Krycka, E. Blackburn, *this proceeding* (2023).
20. W. Schweika, N. Violini, K. Lieutenant, C. Zendler, D. Nekrassov, A. Houben, P. Jacobs, P. Henry, J. Phys.: Conf. Ser. **746**, 012013 (2016).
21. W. Schweika, J. Phys.: Conf. Ser. **211**, 012026 (2010).
22. G. Ehlers, J. Stewart, A. Wildes; P. Deen; K. Andersen, Rev. Sci. Instrum. **84**, 093901 (2013).
23. O. Schärpf, H. Capellmann, Phys. Status Solidi A **135**, 359 (1993).
24. P. Willendrup, and K. Lefmann, J. Neutron Res. 22, 1-16 (2020).
25. P. Willendrup, and K. Lefmann, J. Neutron Res. 23, 7-27 (2021).
26. D. M. Rodríguez, P. Willendrup, W.-T. Lee, A. Backs, F. J. Villacorta, R. Toft-Petersen, M. Morgano, *this proceeding* (2023).
27. P. Böni, D. Clemens, M. Kumar, C. Pappas, Physica B **267-268**, 320 (1999).
28. V. Luschikov, Yu. Taran, Nucl. Instrum. Methods Phys. Res. **228**, 159 (1984).

29. P. Jorba, M. Schulz, D. Hussey, M. Abir, M. Seifert, V. Tsurkan, A. Loidl, C. Pfleiderer, B. Khaykovich, J. Magn. Magn. Mater. **475**, 176 (2019).
30. S. Jaksch, A. Chennevière, S. Désert, *et. al*. Appl. Sci., **11**(8), 3620 (2021).
31. P. Deen, S. Longeville; W. Lohstroh, F. Moreira, G. Fabrèges, L. Loaiza, D. Noferini, Rev. Sci. Instrum. **92**, 105104 (2021).
32. COMSOL Multiphysics® v. 6.1. www.comsol.com. COMSOL AB, Stockholm, Sweden.
33. K. Andersen, R. Cubitt, H. Humblot, D. Jullien, A. Petoukhov, F. Tasset, C. Schanzer, V. Shah, A. Wildes, Physica B **385**–**386**, 1134 (2006).
34. Q. Yea, T. Gentile, J. Anderson, C. Broholm, W.C. Chen, Z. DeLand, R. Erwinb, C. B. Fue, J. Fuller, A. Kirchhoff, J. Rodriguez-Rivera, V. Thampy, T. Walker, S. Watson, Physics Procedia **42**, 206 (2013).
35. L. Schearer, G. Walters, Phys. Rev. **139**, 1398 (1965).
36. A. Petoukhov, V. Guillard, K. Andersen, E. Bourgeat-Lami, R. Chung, H. Humblot, D. Jullien, E. Lelievre-Berna, T. Soldner, F Tasset, M. Thomas, Nucl. Instrum. Methods Phys. Res. A **560**, 480 (2006).
37. W.C. Chen, Md. Hassan, R. Erwin, S. Watson, T. Gentile, G. Jones, Rev. Sci. Instrum. **91**, 105102 (2020).
38. D. Jullien, A. Petoukhov, M. Enderle, N. Thiery, P. Mouveau, U. Hansen, P. Chevalier, P. Courtois, Nucl. Instrum. Methods Phys. Res. A **1010**, 165558 (2021).
39. J. Stewart, K. Andersen, E. Babcock, C. Frost, A Hiess, D. Jullien, J. Stride, J.-F. Barthélémy, F. Marchal, A. Murani, H. Mutka, H. Schober, Physica B **385**–**386**, 1142 (2006).
40. E Babcock, Z Salhi, P Pistel, G Simeoni, A Ioffe, J. Phys.: Conf. Ser. **528**, 012018 (2014).
41. K. Andersen, D. Jullien, A. Petoukhov, P. Mouveau, F. Bordenave, F. Thomas, E. Babcock, Physica B **404**, 2652 (2009).
42. R. Merritt, C. Purcell, G. Stroink, Rev. Sci. Instrum. **54**, 879 (1983).
43. G. Gottardi, P. Mesirca, C. Agostini, D. Remondini, F. Bersani, Bioelectromagnetics **24**, 125 (2003).
44. A. Wildes, Rev. Sci. Instrum. **70**, 4241 (1999).
45. J. Auckett, W.-T. Lee, K. Rule, A. Bosak, C. Ling, Inorganic Chemistry **58**, 12317 (2019).